Morphology-dependent enhancement of arsenite oxidation to arsenate on birnessite-type manganese oxide

Jingtao Hou [a,b,c], Yongjin Xiang [b], Dan Zheng [b], Yuanzhi Li [c], Shengguo Xue [d,e,*], Chuan Wu [d,e,*], William Hartley [f], Wenfeng Tan [a]

[a] College of Resources and Environment, Huazhong Agricultural University, Wuhan 430070, China
[b] School of Environmental and Biological Engineering, Wuhan Technology and Business University, Wuhan 430065, China
[c] State Key Laboratory of Silicate Materials for Architectures Wuhan University of Technology, Wuhan 430070, China
[d] Department of Environmental Engineering, School of Metallurgy and Environment, Central South University, Changsha 410083, China
[e] Chinese National Engineering Research Centre for Control and Treatment of Heavy Metal Pollution, Changsha 410083, China
[f] Crop and Environment Sciences Department, Harper Adams University, Newport, Shropshire TF10 8NB, United Kingdom

HIGHLIGHTS

- As(III) oxidation performance of different birnessite morphologies was investigated.
- Varying morphology from nanosheet to nanoflower significantly promotes As(III) oxidation activity of birnessite.
- Origin of morphology effect on As(III) removal was experimentally and theoretically studied.
- Presence of high oxygen vacancy defect concentration makes adsorption of As(III) on birnessite more favorable.
- Presence of high oxygen vacancy defect concentration in birnessite accelerates the charge transfer from As to Mn atoms.

GRAPHICAL ABSTRACT
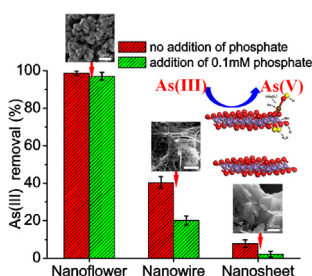
ARTICLE INFO

ABSTRACT

Birnessite-type manganese oxide is a highly efficient oxidant that has been investigated widely for As(III) oxidation. Nevertheless As(III) oxidation rate is inevitably reduced due to favorable adsorption of coexisting ions and As(V) which passivate its surface. In this paper we explore a novel strategy to significantly improve As(III) oxidation performance by controlling birnessite morphology. The batch experiment results show that the nanoflower-like birnessite (Bir-NF) exhibits an incredible improvement in As(III) oxidation activity compared to nanowire-like (Bir-NW) and nanosheet-like (Bir-NS) birnessites. The morphology of birnessite varies from nanosheet to nanoflower not only promotes As(III) oxidation rate from 1.4 to 24.7 $\mu mol\ g^{-1}\ min^{-1}$, but also reduces the adverse effect of adsorption of As(V) and coexisting ions on As(III) removal. The origin of morphology-dependent enhancement of As(III) removal was experimentally and theoretically studied by As(V) adsorption on birnessites, phosphate adsorption kinetics, detection of dissolved Mn^{2+} concentration, average Mn oxidation state, the point of zero charge, and density functional theory (DFT) calculations. The results reveal that significant enhancement of As(III) oxidation activity in Bir-NF as compared to Bir-NW and Bir-NS is attributed to its highly efficient contact between

* Corresponding authors at: Department of Environmental Engineering, School of Metallurgy and Environment, Central South University, Changsha 410083, China (S. Xue and C. Wu).
E-mail addresses: sgxue70@hotmail.com (S. Xue), wuchuan@csu.edu.cn (C. Wu).

As(III) species and manganese oxide, as well as its fast charge transfer from As atom to Mn atom due to its highest oxygen vacancy defect concentration, thus significantly promoting As(III) oxidation activity.

1. Introduction

Arsenic (As) is one of the most common environmental pollutants which can exist in four oxidation states, arsine (-3), arsenic (0), arsenite (+3), and arsenate (+5). Arsenite [As(III)] and arsenate [As(V)] are the two main arsenic species that are found in arsenic-containing wastewater. Arsenite has a greater toxicity but a weaker affinity for adsorbents than As(V), the preoxidation of As(III) to As(V) is regarded as a critical process for decreasing As toxicity and improving total As removal using treatment methods such as adsorption and co-precipitation [1,2]. To date a large number of chemical oxidants have been developed for highly efficient oxidation of As(III) to As(V). These chemical oxidants include ozone [3], chlorine [4] and hydrogen peroxide [2,5,6]. However, the use of such oxidants for As(III) oxidation are not environmentally friendly, and may lead to the generation of toxic byproducts [7], it is therefore highly desirable to explore other alternatives [8].

The octahedral layered birnessite is a type of manganese oxide that has a two-dimensional (2D) layer structure of edge-shared MnO_6 octahedra with exchangeable ions (e.g., Na^+, K^+) and H_2O molecules inside the interlayer [9]. Because of its high redox potential, birnessite-type manganese oxide has been widely investigated as a highly efficient oxidant for preoxidation of As(III) to As(V) [10–14]. It is well known that oxidation of As(III) to As(V) by manganese oxide couples with adsorption of As(V) [14,15]. Experimental and theoretical evidence demonstrates that As(V) adsorption is more favorable than As(III) on manganese oxide surfaces [14–16]. This means that passivation of manganese oxide surfaces originating from adsorption of As(V) is inevitable, which may lead to a decrease in As(III) oxidation [12,17]. In addition, coexisting ions such as phosphate and Mn^{2+} readily occupy its surface active sites resulting in the blocking of As(III) binding and reducing the extent and rate of As(III) oxidation [12,17]. Therefore a novel approach must be sought to promote As(III) oxidation while reducing the unfavorable effects of As(V) and coexisting ions. Over the past decades, several efforts have been reported for improving As(III) oxidation activity using birnessite-type manganese oxide. For example, Yin et al. synthesized nanostructured Co-doped birnessites via substitution of framework Mn ions with Co ions [18]. They discovered that the Co-doped birnessite sample revealed greater As(III) oxidation activity than birnessites without doping. This effect was attributed to the higher standard redox potential of Co^{3+}/Co^{2+} as compared to that of MnO_2/Mn^{2+}. Villalobos et al. prepared acid birnessite samples with low specific surface area (SSA) and high vacancy content [19]. They confirmed that As(III) oxidation rate per unit surface area of the acid birnessite sample was greater than that of birnessite with high SSA and low vacancy content at pH 6.

The process of controlling birnessite morphology to improve its electrochemical and magnetic properties and the catalytic oxidation and purification of environmental pollutants, has attracted much attention [20–22]. For example, in previous work, we compared the catalytic activity of birnessites with nanoflower, nanowire and nanosheet morphologies, and observed that nanoflower-like birnessite showed significant catalytic activity for benzene oxidation compared to nanowire-like and nanosheet-like birnessites [22]. Nevertheless, there are no reports in the literature as to the effect of birnessite morphology on the oxidation of As(III) to As(V). Here, nanoflower, nanowire and nanosheet birnes-site morphologies were used to oxidize As(III) to As(V). For the first time, we observed the morphology-dependent enhancement of As(III) oxidation activity by birnessite. Compared to nanowire-like and nanosheet-like birnessites, nanoflower-like birnessite not only has the greatest As(III) oxidation rate, but can also resist the adverse effect of As(V) and coexisting ions on As(III) removal. We combine both experimental and theoretical evidence to reveal the origin of morphology-dependent enhancement of As(III) oxidation by birnessite.

2. Experimental section

2.1. Sample preparation

Nanoflower-like birnessite was prepared by a facile hydrothermal reaction between $Mn(NO_3)_2$ (50 wt%) and $KMnO_4$ with $Mn(NO_3)_2/KMnO_4$ molar ratio of 2 at 50 °C for 48 h as described in our previous work [22]. Nanowire-like birnessite was prepared by a hydrothermal reaction between $MnSO_4$ (0.11 g) and $KMnO_4$ (0.6 g) at 240 °C for 24 h as described in the literature reported by Liang et al. [23]. The nanosheet-like birnessite sample was prepared via a facile hydrothermal reaction with $KMnO_4$ (0.948 g) at 240 °C for 24 h as described in the literature reported by Duan et al. [21].

2.2. Batch experimental procedures

Batch experiments of As(III) oxidation on birnessites with different morphologies was performed in a water-bathing oscillator with a setting velocity of 160 rpm at 25 °C. A 10 mmol L^{-1} As(III) stock solution was prepared by dissolving 0.8 g $NaAsO_2$ into distilled water (100 mL). The simulated 0.1 mmol L^{-1} As(III) wastewater was obtained by stepwise dilution of $NaAsO_2$ stock solution using a buffer solution (pH 6.0). Details of the batch experimental procedures are as follows.

Birnessite (0.03 g) was added to a 0.1 mmol L^{-1} As(III) solution (50 mL). During the period of As(III) oxidation, suspensions (2.0 mL) were pipetted into a centrifuge tube (10 mL) at specific intervals, diluted to 8.0 mL with distilled water, and centrifuged at 5000 rpm for 10 min. To investigate the effect of coexisting As(V), phosphate, and Mn^{2+} on As(III) removal, 0.1 mmol L^{-1} $NaH_2AsO_4·7H_2O$, NaH_2PO_4, and $Mn(NO_3)_2$ were respectively added into the initial As(III) solution. The effect of NaH_2PO_4 and $Mn(NO_3)_2$ on As(III) removal was performed by respectively adding 0.1, 1.0, and 10 mmol L^{-1} into the initial As(III) solution at pH 6.0. The effect of birnessite dosage was carried out by setting the dosages to 0.2, 0.4, 0.6, 0.8, and 1.0 g L^{-1} nanoflowers at pH 6.0. The effect of pH on As(III) removal was conducted by using buffer solutions of pH 4.7, 6.0 and 9.16, respectively. The acetate acid/sodium acetate buffer system was used for adjusting pH to 4.7 and 6.0. Sodium carbonate/sodium bicarbonate buffer system was used for adjusting pH to 9.16. The preparation details of these buffer solutions are described in previous work [17]. The change of pH values in arsenic solution was recorded in different reaction period of 0 min, 30 min, and 24 h at different buffer systems. The result reveals that the pH has no change during the entire reaction, indicating that the buffer systems used in this work are stable (Fig. S1, Supporting information).